DRD Line No. SE-5

DOE/JPL-955164-78/4
Distribution Category UC-63

DEVELOPMENT OF ECONOMICAL IMPROVED THICK FILM SOLAR CELL CONTACT

BERND ROSS and DAVID MENTLEY

BERND ROSS ASSOCIATES
2154 Blackmore Ct.
San Diego, CA 92109

QUARTERLY REPORT NO. 1

January 1979

Contractual Acknowledgement

The JPL Low-Cost Silicon Solar Array Project is sponsored by the U.S. Department of Energy and forms part of the Solar Photovoltaic Conversion Program to initiate a major effort toward the development of low-cost solar arrays. This work was performed for the Jet Propulsion Laboratory, California Institute of Technology by agreement between NASA and DOE.

DRD Line No. SE-5

DOE/JPL-955164-78/4
Distribution Category UC-63

DEVELOPMENT OF ECONOMICAL IMPROVED THICK FILM SOLAR CELL CONTACT

BERND ROSS and DAVID MENTLEY

BERND ROSS ASSOCIATES
2154 Blackmore Ct.
San Diego, CA 92109

QUARTERLY REPORT NO. 1

January 1979

Contractual Acknowledgement

The JPL Low-Cost Silicon Solar Array Project is sponsored by the U.S. Department of Energy and forms part of the Solar Photovoltaic Conversion Program to initiate a major effort toward the development of low-cost solar arrays. This work was performed for the Jet Propulsion Laboratory, California Institute of Technology by agreement between NASA and DOE.

TABLE OF CONTENTS

LIST OF FIGURES

1.0 SUMMARY

During the first quarter of this investigation, materials were surveyed to provide candidates for an all metal electrode paste system. These consisted of a major constituent metal powder, a low melting metal powder suitable for a liquid phase sintering medium, and a powder material suitable as an etchant for silicon dioxide at sintering temperatures. By means of thermal gravimetric analysis a suitable binder was identified for low temperature fired inks.

The all metal ink concept was first demonstrated with the silver system to avoid the problems of limited process windows encountered with base metal systems.

A number of solid materials capable of selectively etching silicon dioxide at modest temperatures were identified. One of these, silver fluoride, has yielded very good results, wetting the silicon surface after removing a thick (3000Å) silica layer. Silver pastes containing the above materials have been prepared. A paste with silver fluoride was screened onto N-type silicon with 5Ωcm resistivity. The resulting contact pads had excellent adhesion but were not electrically ohmic. Metallurgically, these contacts have equal or better grain structure as commercial inks fired at the same temperatures. Another metal ink paste, incorporating boric acid, gave substantially lower resistances, however would not pass a 1-hour boiling DI water immersion without losing scratch resistance.

2.0 INTRODUCTION

The potential for economy and efficiency has been demonstrated for the thick film metallization process using screen printing for solar cell electrodes. However, process reliability and materials economy remain deficient. It is believed that these deficiencies can be removed by the use of ink formulations designed specifically for silicon solar cells, departing from ceramic technology tradition and utilizing all metal systems. The objectives of this investigation are as follows:

1. Eliminate the glass frit which has been the conventional liquid phase sintering medium and adhesive for metallization inks.

2. Provide an appropriate metal which can serve as the liquid phase sintering medium.

3. Find a chemical constituent which effectively removes the native oxide from the silicon during the firing step, which can be made part of the ink, and which either becomes fugitive or remains an inert part of the matured metallization.

4. Maintain cognizance of the cost objectives of the LSA Project in selecting materials and processes.

3.0 METAL SYSTEMS CONSIDERATIONS

A large number of phase diagrams of binary metal systems were examined. Several systems were selected as potential candidates based upon conductivity, compatibility with silicon, process, solderability and cost. Process factors included mutual solubilities, temperature requirements and toxicity. Solubility curves were plotted from the phase diagrams for several systems. Metal system candidates included copper/tin, copper/zinc, nickel/zinc, cerium/copper, cerium/nickel, silver/tin, silver/lead, silver/antimony and silver/bismuth.

It is expected that the requirements for good liquid phase sintering are: good wetting of the major constituent powder grains (copper, nickel, or silver) by the frit metal liquid, reasonable solubility of the major constituent in the liquid metal, and generally compatible phase diagrams without intermetallics. Some solid solubility curves are plotted in Figures 1,2, and 3. While silver in lead and copper in zinc appear well-behaved with increasing solubilities with temperature, the four experimental points given for silver in tin are puzzling and appear to indicate a retrograde solubility.

Initial experiments with base metal powders (copper-zinc and copper-tin) carried out in neutral atmospheres or forming gas showed both lacking adhesion and no sintering. This was attributed to oxide problems on silicon surfaces as well as on powder grains preventing wetting, along with excessive copper grain size. It was therefore decided to investigate SiO_2 removal, and to utilize

a major constituent powder with readily available optimal size ranges and generally well-known and well-behaved properties as a test vehicle for the all metal ink system. Since silver met these objectives, it was considered the best choice.

Fig. 1
SOLID SOLUBILITY OF SILVER IN LEAD

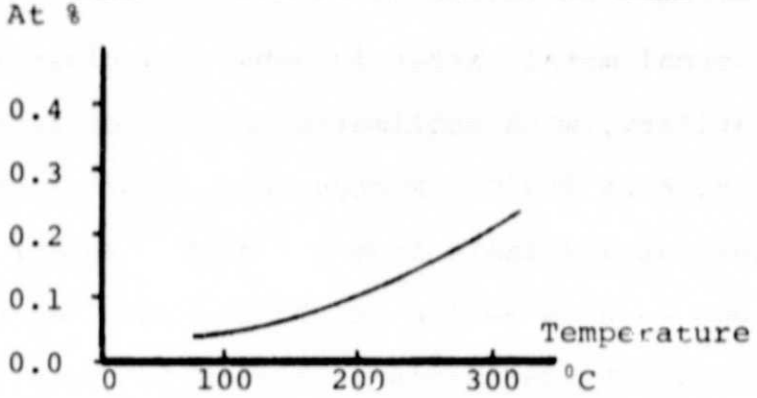

(Data taken from Ref. 1, p.38)

Fig. 2
SOLID SOLUBILITY OF COPPER IN ZINC

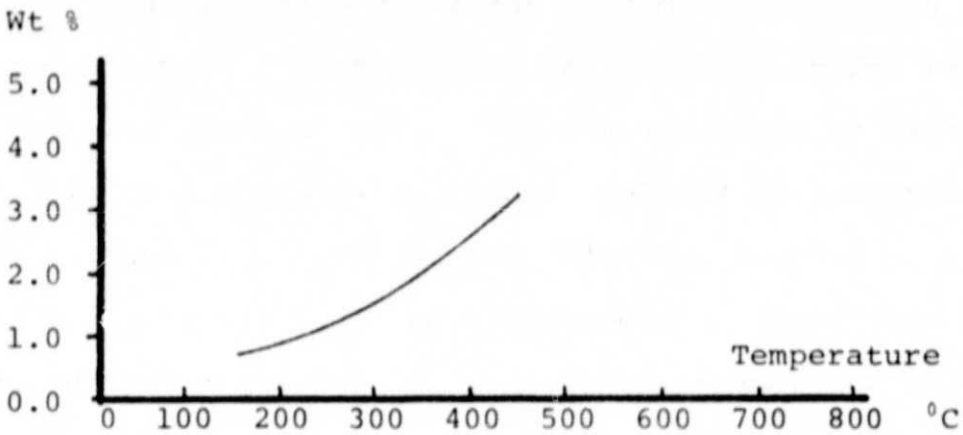

(Ibid,p. 651)

Fig. 3
SOLID SOLUBILITY OF SILVER IN TIN

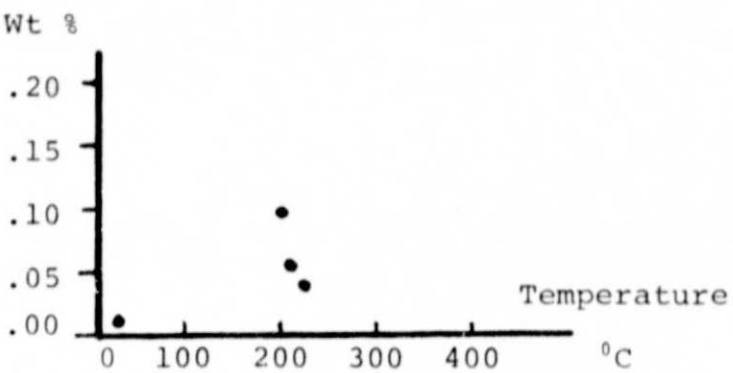

(Ibid,p.52)

4.0 Metal Ink Binder

The binder in the normal metal pastes is ethyl cellulose which has a very low volatility, with sublimation being complete only at temperatures as high as 800°C. Fortunately, a proprietary acrylic based binder was available from the subcontractor which depolymerizes at temperatures as low as 225°C. This can be seen from the combined TGA/DTA traces in Figure 4. This shows the weight loss (or gain) on the trace labeled TGA (thermal gravimetric analysis.) The differential thermal analysis indicates exothermic (+) and endothermic (-) reactions. These curves provide valuable information about the chemical and physical reactions taking place as the temperature is swept from room temperature to the desired upper limit. A check was made with this instrument on the decomposition temperature of silver fluoride. Figure 5 shows the TGA/DTA trace. A temperature of 470°C was found for decomposition. The dip of the DTA line below the average trace at 435°C indicates melting in agreement with the literature.[2]

PART NO. 990092

RUN NO. DATE 10-6-78 OPERATOR D M SAMPLE V5005 (BINDER) ATM @ AIR FLOW RATE 3 CU FT/HR	T-AXIS SCALE mv in 0.8 PROG RATE C min HEAT COOL ISO SHIFT in 0	DTA DIF SCALE 4.0 WEIGHT mg REFERENCE	TGA SCALE mg in 5.0 SUPPRESSION mg WEIGHT mg 30.0 TIME CONST	TMA SCALE mils in MODE SAMPLE SIZE LOAD g dY (10X) (mils min) in

ORIGINAL PAGE IS OF POOR QUALITY

DuPont Instruments

MEASURED VARIABLE

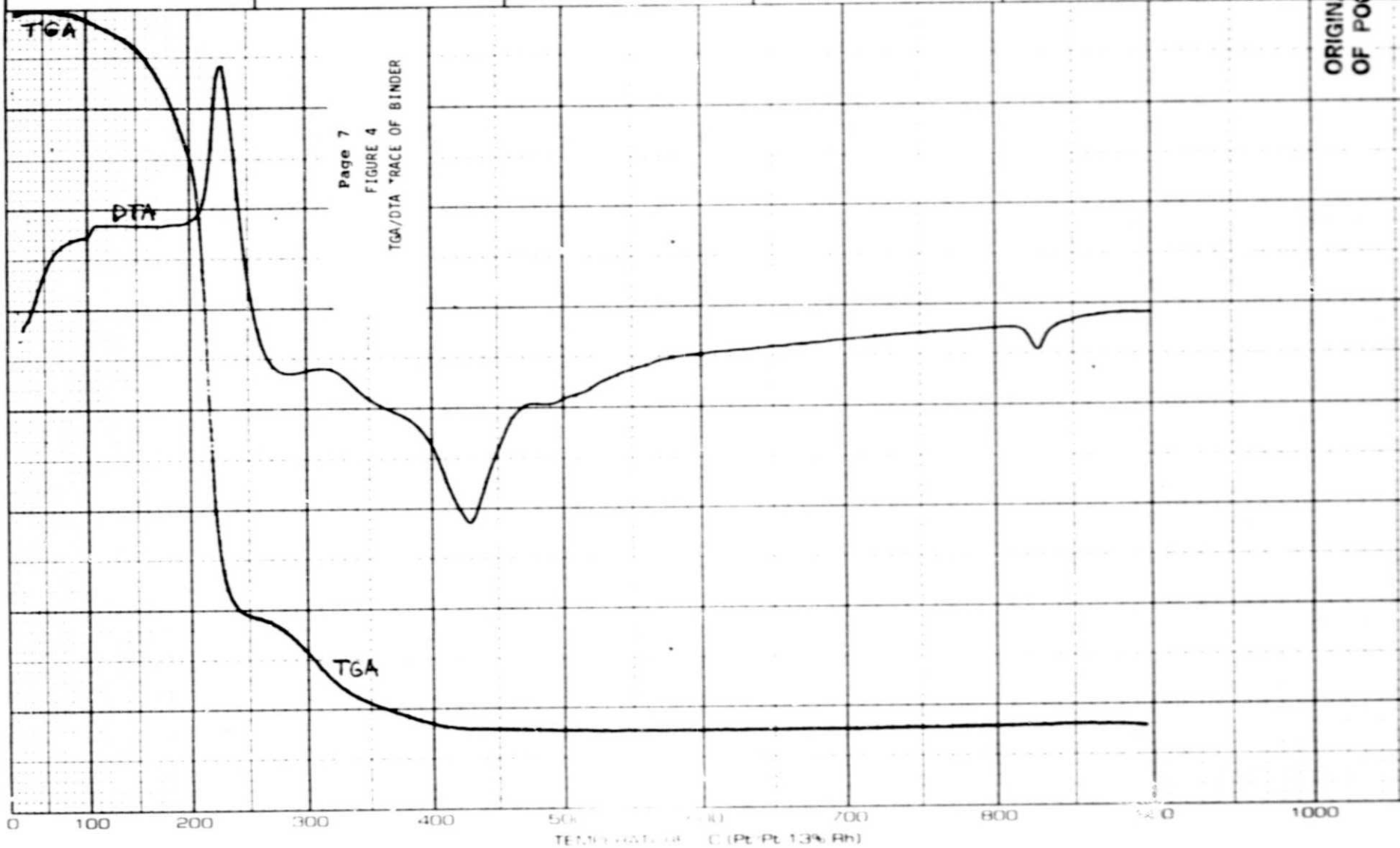

Page 7
FIGURE 4
TGA/DTA TRACE OF BINDER

TEMPERATURE °C (Pt-Pt 13% Rh)

PART NO. 990092

RUN NO ___ DATE ___
OPERATOR DM
SAMPLE
SILVER FLUORIDE
A F
ATM AIR
FLOW RATE 3 CUFt/hr

T AXIS
SCALE 0.8
PROG RATE 15
HEAT COOL ISO
SHIFT 0

DTA DS
4.0

TGA
5.0
30.0

TMA
SCALE
MODE
SAMPLE SIZE
LOAD g

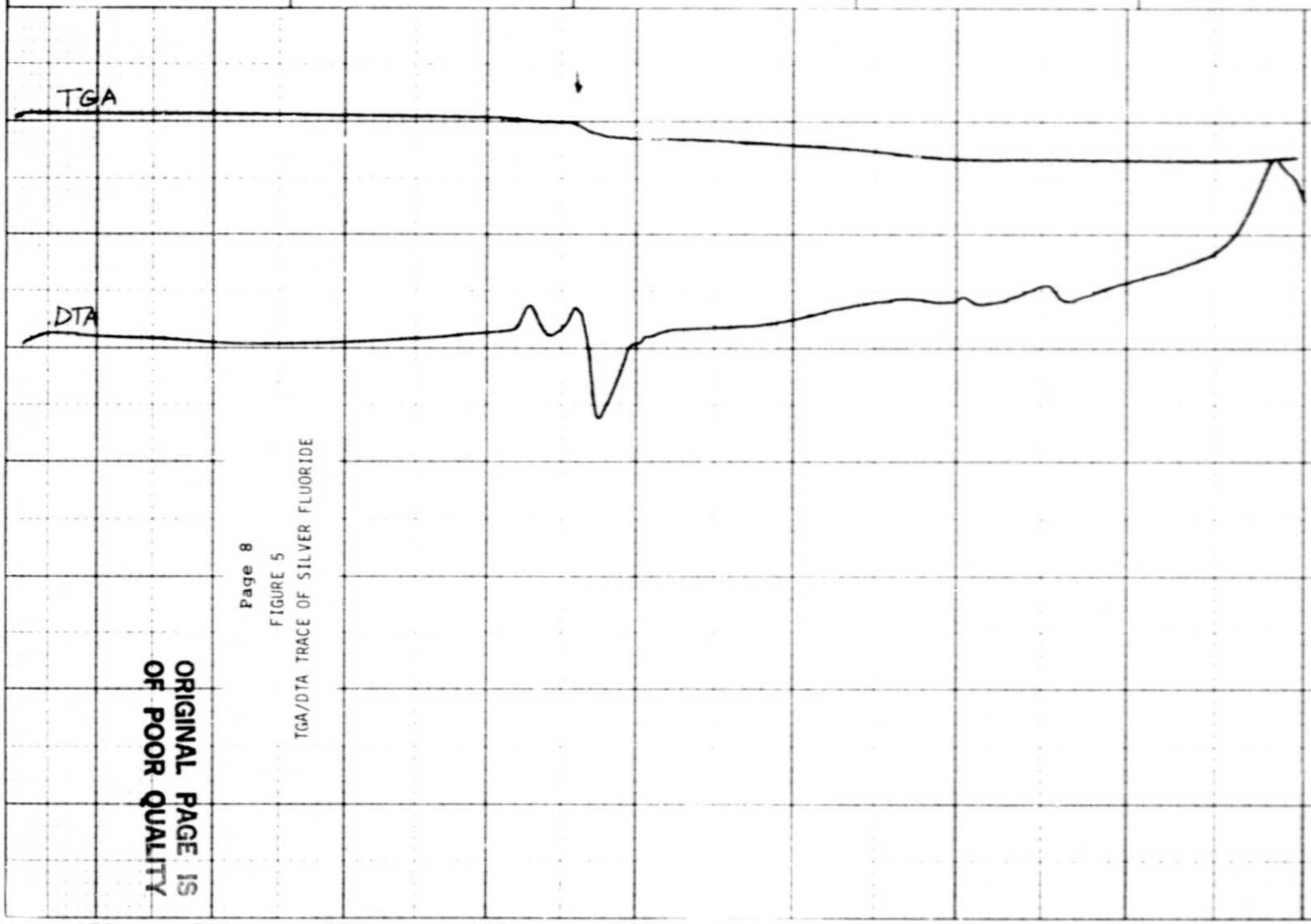

100 200 300 400 500 700 800 900 1000 11

TEMP (Pt/Pt 13% Rh)

FIGURE 5
TGA/DTA TRACE OF SILVER FLUORIDE

5.0 Considerations on Silicon Dioxide Removal

Silicon dioxide is easily removed with HF in an aqueous solution or by dry,hot fluorine, according to:

$$4\ HF + SiO_2 \rightarrow SiF_4 + 2H_2O$$

$$2F_2 + SiO_2 \xrightarrow{\Delta} SiF_4 + O_2$$

Since the use of HF is not convenient, we looked for fluorine-containing compounds which had low decomposition or melting temperatures and could be incorporated in the metal paste. The most attractive material appeared to be silver fluoride (AgF) which according to the literature, decomposes at 435°C. Others ordered included zinc fluoride (ZnF_2), aluminum fluoride (AlF_3), ammonium fluoride (NH_4F) and ammonium bifluoride (NH_4HF_2). The metal fluoride salts are expected to decompose with the fluorine becoming fugitive in the nascent state (F), causing it to be highly reactive. The cation is left behind reduced to the metallic form and is expected to combine with the other metallic ink constituents. This reaction would go in accordance with

$$4AgF + SiO_2 \xrightarrow{\Delta} SiF_4 + 4Ag + O_2$$

In the ammonium salt decomposition the products are gaseous, ammonia, fluorine and in the case of NH_4HF_2, anhydrous hydrofluoric acid.

Since the metallic hydrides, titanium hydride and zirconium hydride, act in a very similar manner, releasing highly reactive

nascent hydrogen and leaving the metal behind, these hyrdrides were tried as well.

6.0 Silicon Dioxide Removal Experiments

Polished silicon wafers of N type material and a resistivity of 5Ωcm were oxidized in air at a temperature of 1100°C for 30 minutes. The resulting silica layers gave uniform interference colors of reddish-purple and were estimated to be 2500Å (0.25μm) thick. Subsequent SEM photographs showed the thickness to be closer to 3000Å (0.3μm). The rationale for growing such a thick layer of SiO_2 was the ease with which the efficacy of an etchant material could be judged in this system. While the thickness of the native oxide is probably only a few atomic layers (10 - 20Å), it is quite difficult to determine the existence of such layers by unsophiscticated means.

A small quantity of pure fluorine containing material was placed in the center of the oxidized wafer. The wafer was put on a Kulicke-Soffa bonder heater stage and observed with a binocular microscope. The heater stage was set to a pre-determined temperature. This temperature was usually about 100°C above the estimated decomposition temperature. The estimate was based upon our TGA/DTA measurements and values obtained from the literature.

7.0 Ammonium fluoride

Figure 6 shows the TGA/DTA traces for ammonium fluoride (NH_4F). The TGA trace illustrates that weight loss occurs almost immediately, with the slope becoming quite steep at 150°C. While there are several inflection points, further emphasized by the structure apparent on the DTA trace, the weightloss is 71% complete at 250°C and 100% at 450°C. The structure exhibited in the DTA of Figure 6 is not understood. According to Berzelius[3], NH_4F melts prior to decomposition, a phenomenon not noted by other references. The same reference points out that dissociation of ammonium fluoride proceeds according to $NH_4F \rightarrow NH_3 + HF$. Similarly, the reference asserts that NH_4F will dissociate into NH_4HF_2 and $NH_3\uparrow$ in the presence of water.

Figure 7 shows an electron micrograph taken on a Cambridge SEM 1700X magnification, showing the boundary between the virgin layer and the portion covered with ammonium fluoride. A light microscope examination showed a dark residue, whose nature remains unknown.

PART NO. 990092

RUN NO ___ DATE 11-8-78
OPERATOR DM
SAMPLE AMMONIUM FLUORIDE NH_4F
ATM AIR
FLOW RATE 3 CU FT/HR

T AXIS
SCALE 0.8
PROG RATE C/min 25
HEAT COOL ISO
SHIFT in 0

DTA
SCALE 4.0

TGA
SCALE mg in ~12
SUPPRESSION mg
WEIGHT mg 85

TMA
SCALE mils in
MODE
SAMPLE SIZE
LOAD g
dY (10X) (mils/min)/in

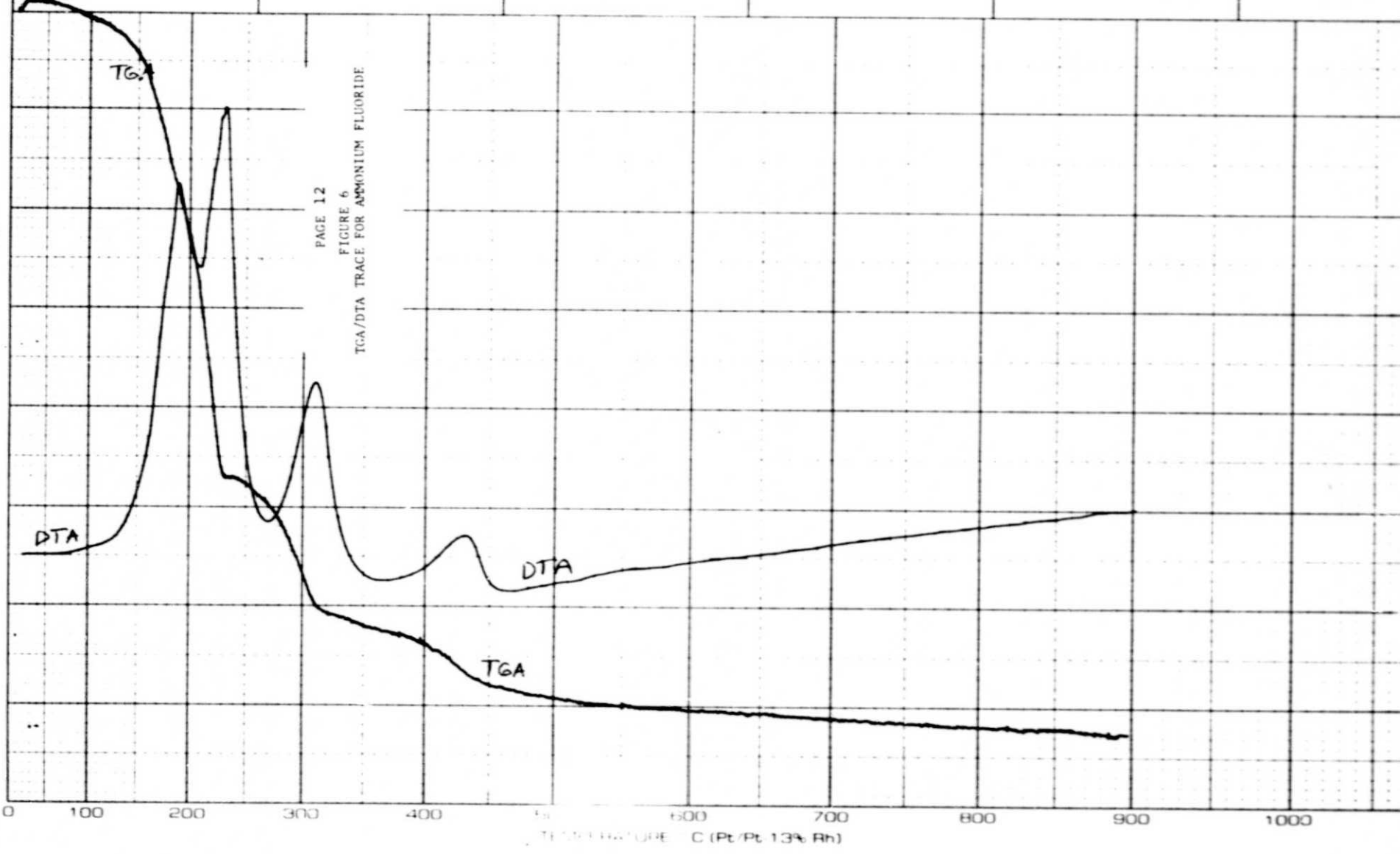

PAGE 12
FIGURE 6.
TGA/DTA TRACE FOR AMMONIUM FLUORIDE

DUPONT Instruments

MEASURED VARIABLE

ORIGINAL PAGE IS
OF POOR QUALITY

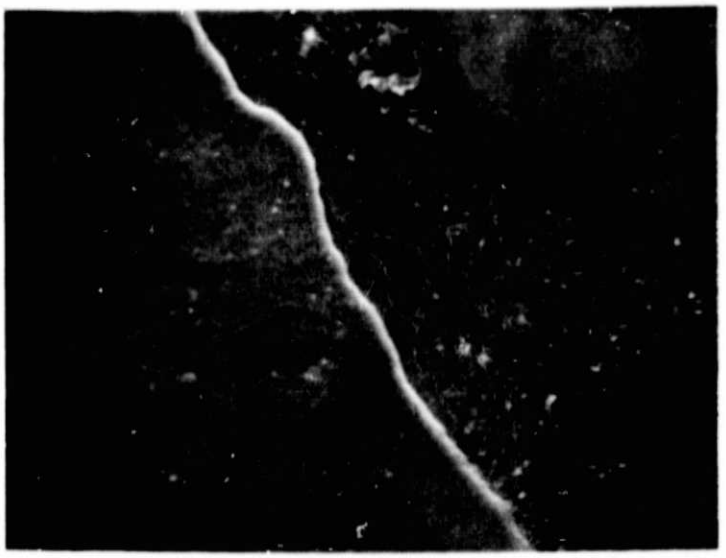

Figure 7. SiO_2 3000Å thick on silicon, left half of photomicrograph. Right portion etched by ammonium fluoride NH_4F at 600°C. Taken on Cambridge SEM at 1700X.

8.0 Ammonium bifluoride (NH_4HF_2)

Figure 8 shows the TGA/DTA traces of ammonium bifluoride to be very similar to those of ammonium fluoride. The action upon silicon dioxide was also similar, and therefore no electron micrograph is shown.

9.0 Teflon^R

Figure 9 shows the TGA/DTA trace for Teflon^R. The continuous rise in the TGA trace is possibly due to the aerodynamics of a different crucible, experiencing lift in the chimney of the apparatus,which would be interpreted as weightloss. Melting occurs at 320°C (DTA) and decomposition is apparent from the

PART NO. 990092

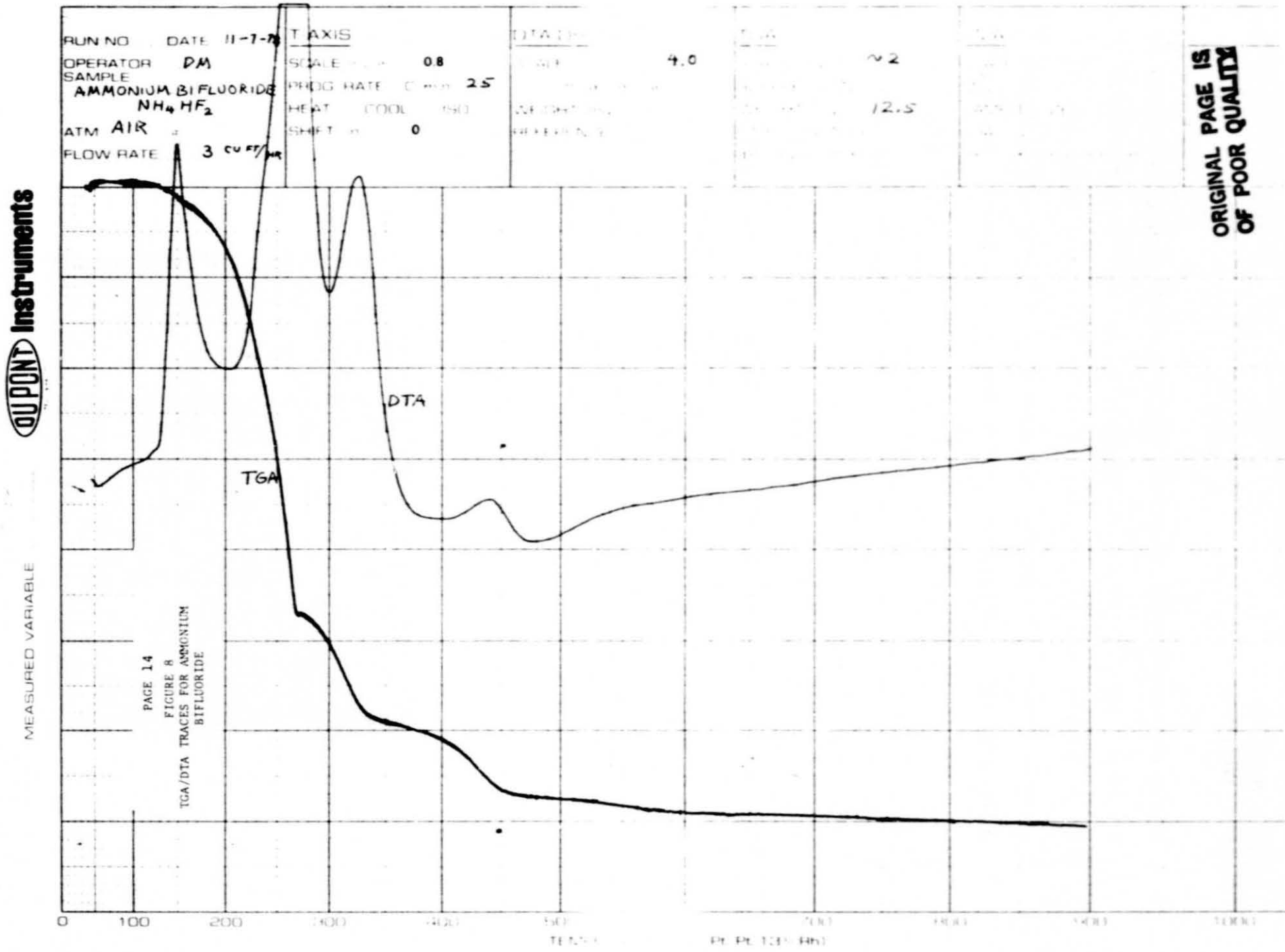

ORIGINAL PAGE IS OF POOR QUALITY

DUPONT Instruments

PAGE 14

FIGURE 8
TGA/DTA TRACES FOR AMMONIUM BIFLUORIDE

PART NO. 990092

RUN NO ____ DATE 11-9-78
OPERATOR DM
SAMPLE DLX 6000 (TEFLON®)
ATM AIR @ ____
FLOW RATE 3 CU FT/HR

T-AXIS
SCALE mV in 0.8
PROG RATE C/min
HEAT ____ COOL ____ ISO
SHIFT in 0

DTA
SCALE 4.0
WEIGHT mg
REFERENCE

TGA
SCALE mg/in 5.0
SUPPRESSION mg
WEIGHT mg 35.6
TIME CONST sec
dY (mg/min) in

TMA
SCALE mils/in
MODE
SAMPLE SIZE
LOAD g
dY (10X) (mils/min)/in

TGA

DTA

0 100 200 300 400 500 600 700 800 900 1000

TEMPERATURE °C (Pt/Pt-13% Rh)

MEASURED VARIABLE

PAGE 15

FIGURE 9. TGA/DTA TRACES FOR TEFLON® POWDER

DUPONT Instruments

weightloss beginning at 500°C and being complete at 630°C. Figure 10 is an SEM photo of the interface of the attacked versus the non-attacked portions of the oxidized wafer. Optical microscopy again revealed a considerable amount of residue. There is an indication on the SEM that the silicon surface may have been attacked as shown in the apparent cratering on the left side of the photo.

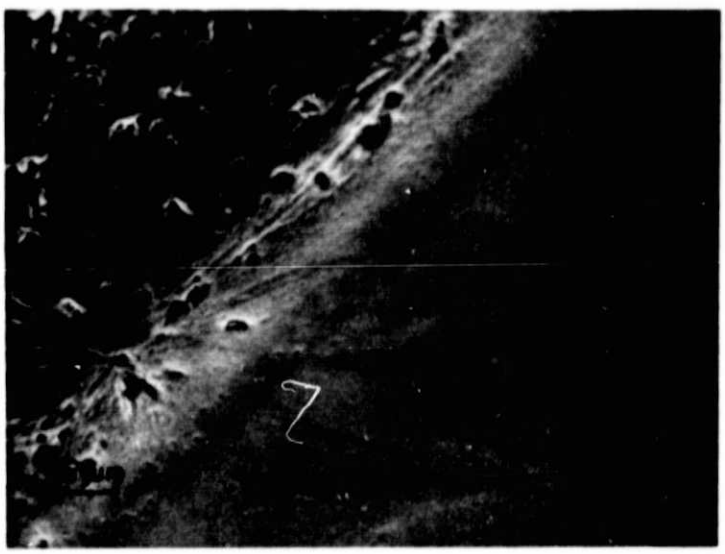

Figure 10. SiO_2 3000 Å thick on silicon, right half of photo. Left half etched by decomposed Teflon® at 600°C. Taken on Cambridge SEM at 1600X.

10.0 Silver fluoride AgF

Only a small quantity of silver fluoride was obtained due to its rather high price (over $6/g). It was later established that this high price is not warranted by material and labor costs.[4] An attempt to obtain electronmicrography of a silver fluoride grain proved to be impossible as the 10 KeV (100μA cathode current) electron beam decomposed the specimen grain in considerably less than a minute at 1000X magnification.

Figure 11 shows an SEM photo of a typical silver grain resulting from AgF dissociation at 500°C on an oxidized silicon wafer. Magnification is 4000X. It can be seen that a moat has been carved out of the silica around the original silver fluoride grain. The resulting silver blob has thinned down markedly near its periphery, making a low contact angle with the silicon, a condition expected when good wetting is demonstrated.[5] The continuous metal surface is probably due to the catalytic action of the very fine particles generated by the decomposition of the silver fluoride, as well as the catalytic action of the freshly exposed silicon crystal surface. To verify the nature of the deposited material, a series of photomicrographs was taken at increasing magnification. The backscatter mode of the Cambridge SEM was employed, providing a higher yield of electrons from the surface of materials with a high atomic number relative to the darker background (Ag Z=47 : Si Z=14). Figure 12 shows a different portion of the same sample from which Figure 11 was taken, at 1600X magnification. Figure 13 shows a portion of Figure 12 at 3700X magnification, again employing the backscatter

mode. Figure 14 shows the same region as Figure 13, but as a silver elemental map using the L_{α} (2.98 KeV) line X-ray fluor escence. The open areas on the solid silver portions are due to the finite integration time utilized. The sparse number of dots, where no silver is expected, is from noise and possibly some contamination.

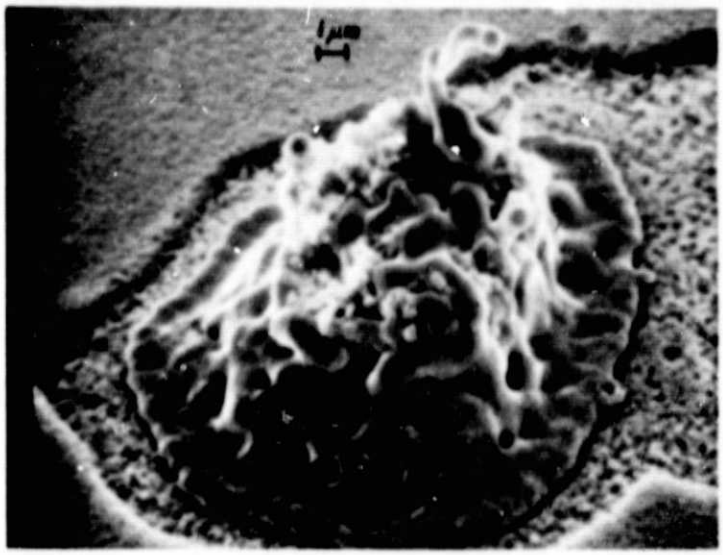

Figure 11. AgF on SiO_2 (3000 Å thick) at 500°C. Vicinity of reduced silver shows etching action on SiO_2. Good wetting is indicated by low angle of periphery profile. Cambridge SEM at 4000X.

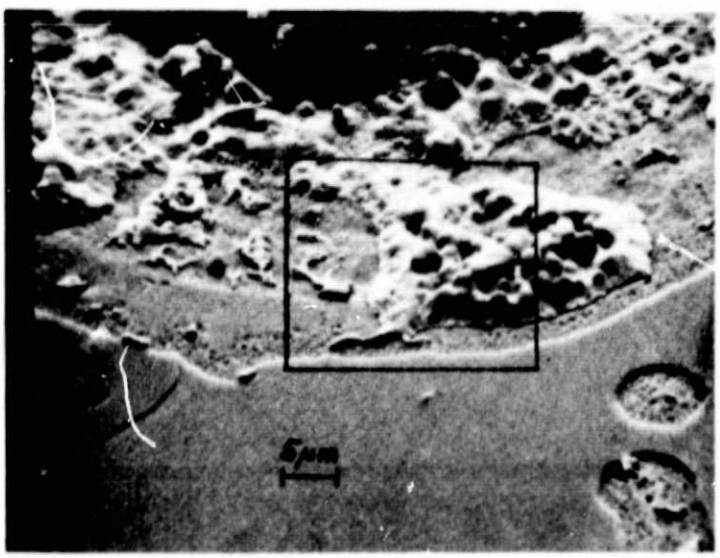

Figure 12. Different portion of same sample as above. Taken in back-scatter mode at 1500X.Cambridge SEM.

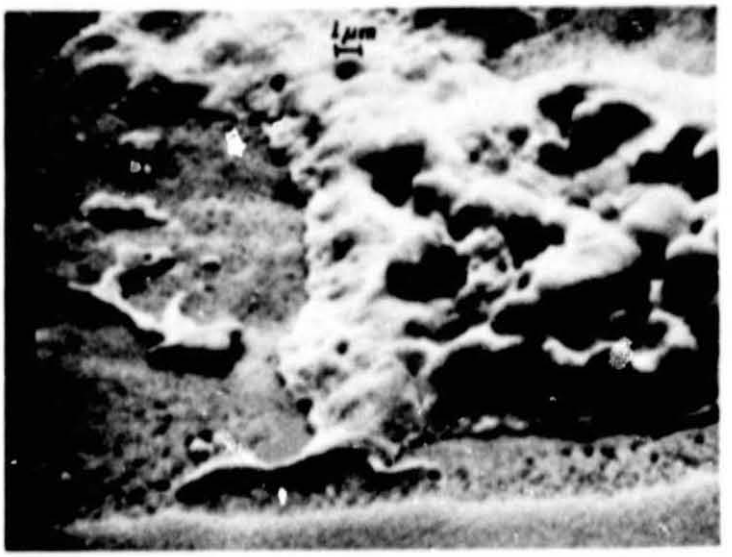

Figure 13. Same sample as Figures 12 and 11 (AgF) taken in backscatter mode on Cambridge SEM at 3700X.

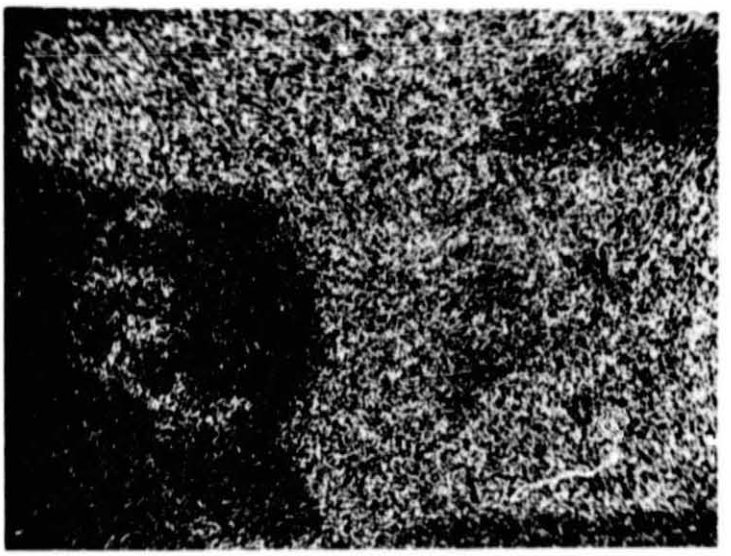

Figure 14. Same sample as Figure 13 showing silver map of region above. Cambridge SEM 3700X 2.98KeV Lα. Integration time 1000 sec.

Figure 15 shows the pressure in atmospheres over silver fluoride at various temperatures. The curves were plotted from the two equations[4] shown on the figure.

In addition to the above, the following were tried, all at a temperature of 600°C.

Aluminum fluoride AlF_3

Zirconium hydride ZrH_2

Titanium hydride TiH_2

There was no evidence of oxide removal discernible in the above materials.

Zinc fluoride ZnF_2

The zinc fluoride was evidently effective in removing the silicon oxide, however, it left behind a large amount of dark residue, probably ZnO. Since the other materials showed more promise, it was decided to abandon the above.

Fig. 15

VAPOR PRESSURE OVER SILVER FLUORIDE

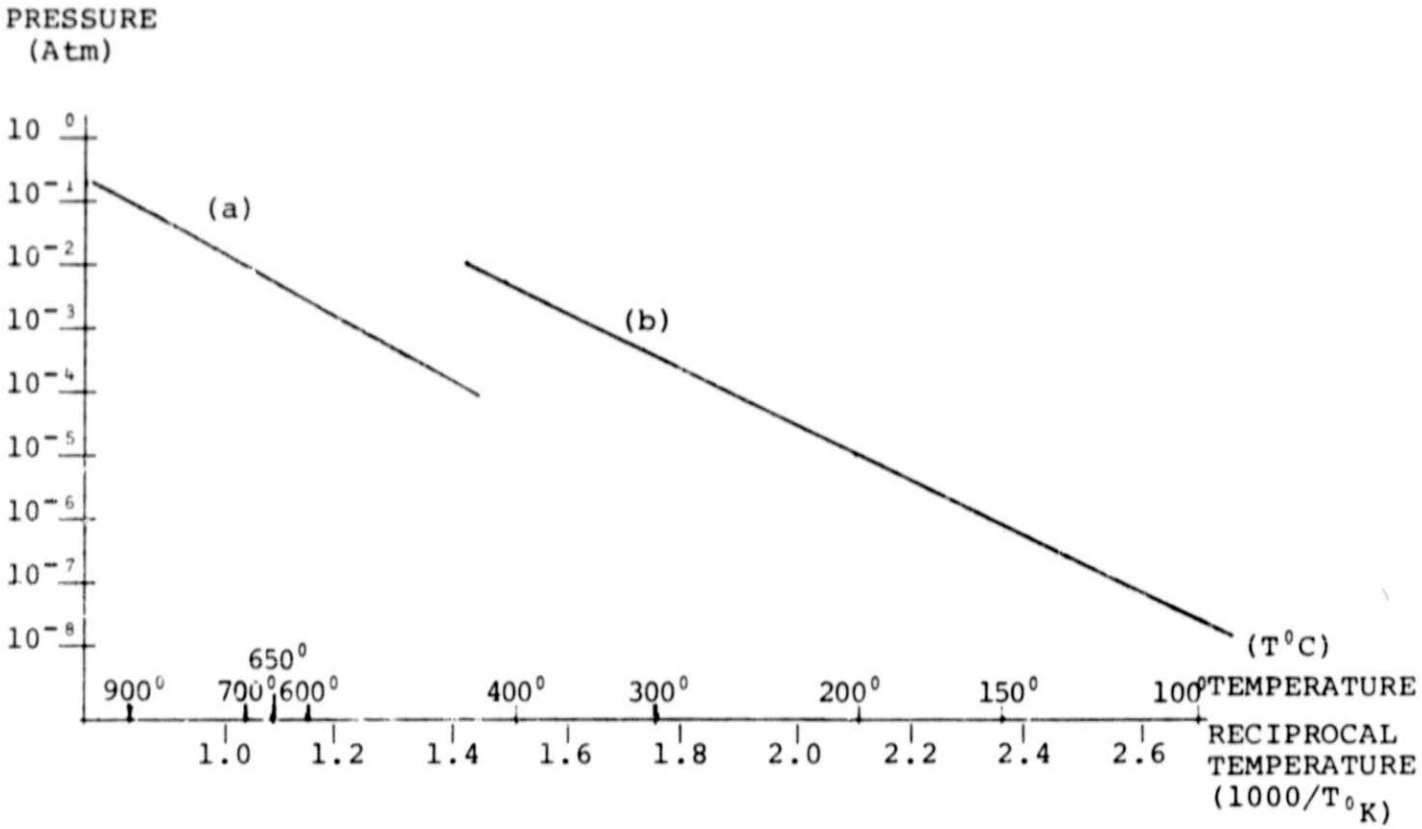

Fig.15 Vapor pressure over a) liquid silver fluoride (AgF) and b) solid silver fluoride (AgF)

(a) above liquid AgF $\quad \ln P_{atm} = -0.937 \cdot 10^4/T_{°K} + 4.78$ for $854^{\circ} < T < 1024^{\circ}K$

(experimental, from reference 6)

(b) above solid AgF $\quad \ln P_{atm} = -1.023 \cdot 10^4/T_{°K} + 10.07$ for $T \leq 708^{\circ}K$

(calculated, from reference 6)

11.0 Silver Paste Experiments

Approximately twelve different experimental pastes were fabricated. The initial paste, consisting of 5 wt%* AgF and 95 wt%* silver powder of particle size ~0.1μm gave good results, but had poor initial rheological properties and continued to deteriorate. This was most likely a function of the extremely small particle size which provides a large area of grain surface, which in turn reduces the lubricating action of the resin binder causing the viscosity to increase.

Subsequently, a coarser silver consisting of powder and flakes was used and a masterpaste was compounded. The masterpaste contains the normal ingredients of metal powder and binder and allows the rapid preparation of a series of pastes to which only the silicon oxide scavenger is added.

Inks containing ammonium fluoride, bifluoride and Teflon^{R} had inadequate adhesion at all temperatures tried (600^{0}C to 750^{0}C.) The criterion was our ability to scrape the electrode off with a single-edged razor blade. In another test, 0.1" squares were soldered with 63-37 tin lead solder. Leach resistance was good and all samples were quickly wetted with solder. However, the Teflon^{R} additive electrodes could be pried off the wafer after soldering, in contrast to the silver fluoride electrodes. Coverage of the silver fluoride compounded electrodes looked good.

Figures 16, 17, 18, and 19 show a sequence of SEM photos of S012 ink paste prepared with 10 wt% added AgF fired at 750^{0}C for five

* Here and throughout report, % refers to wt% of ink solids, only.

minutes. Figure 16 was done at the low magnification of 17X. Figure 17: 420X magnification, Figure 18: 1700X magnification, Figure 19: 4200X magnification. The ridges on the print in the Figures 16 and 17 are due to the paste rheology. It should be noted that the addition of Teflon^{R} powder had a beneficial effect upon the ink rheology. Figures 18 and 19 show that there is a considerable sintering action in this all metal ink even though no liquid phase sintering medium was used. This may be due to the finely divided silver particles from the Ag_2F dissociation.

On the other hand there is considerably less visible wetting action in these photos. It is plausible that wetting occurs under the grains and the tenacious adhesion tends to support this view.

It is interesting to compare the sintering action obtained in this experiment with that on a production solar cell (Figure 20) employing a commercial lead oxide based glass frit ink. The magnification of the glass frit sample is almost twice that of the all metal system (8000X: 4200X) and the grain development and interlocking are excellent. The firing temperatures of the two inks are comparable. (All metal ink: 750^{0}C, commercial fritted ink 700^{0}C).

12.0 FURTHER EXPERIMENTS

In order to eliminate the Schottky type barrier referred to in

the next section under electrical measurements, a paste (S018) was prepared containing 3 wt% boric acid (H_3BO_3) in addition to 5 wt% silver fluoride (AgF) and screened onto p-type wafers of 1 to 3 Ωcm solar cell material. The resistance measurement indicated the barrier to be attenuated (refer to electrical measurements). Subsequently, a wafer with the boron containing ink along with an identical screened contact except for the boron addition (S009) was boiled in de-ionized water for one hour. Both wafers were then subjected to an adherence test involving an Exacto knife. The contact with the H_3BO_3 addition could be scraped off with little difficulty whereas the "undoped" contact survived the test.

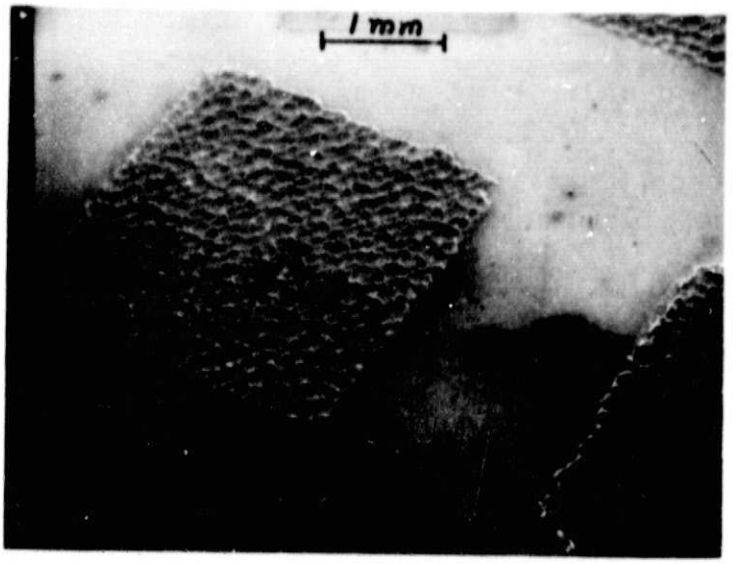

Figure 16. Print with SO12 (10% AgF). Pads are 0.100" X 0.100" spaced 0.050", on polished silicon. Fired at 750°C temperature peak for 5 min. Cambridge SEM at 17X.

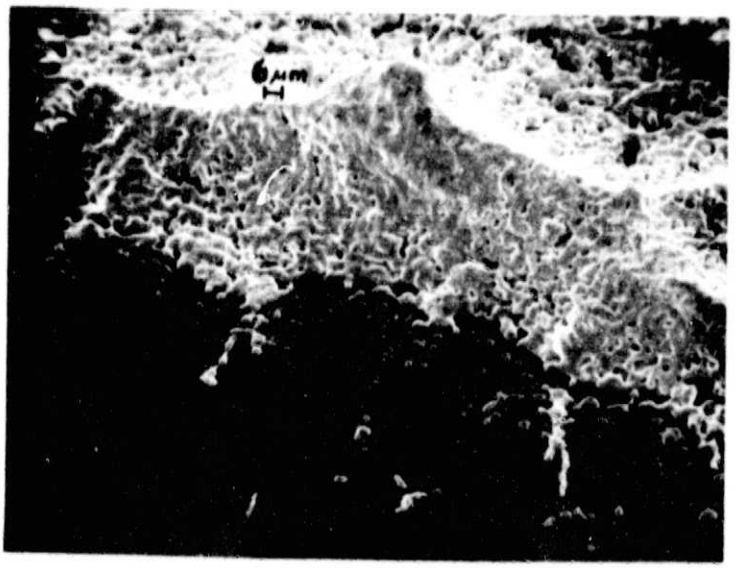

Figure 17. Same as Figure16 magnification 412X. Ridges are reproduction of screen mesh.

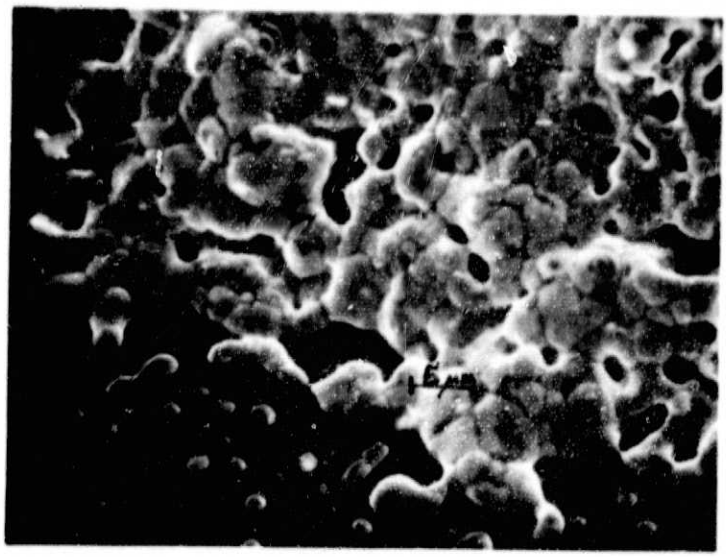

Figure 18. Same as Figures 11 and 12 except magnification 1700X. Note contiguous grain showing dense sintering.

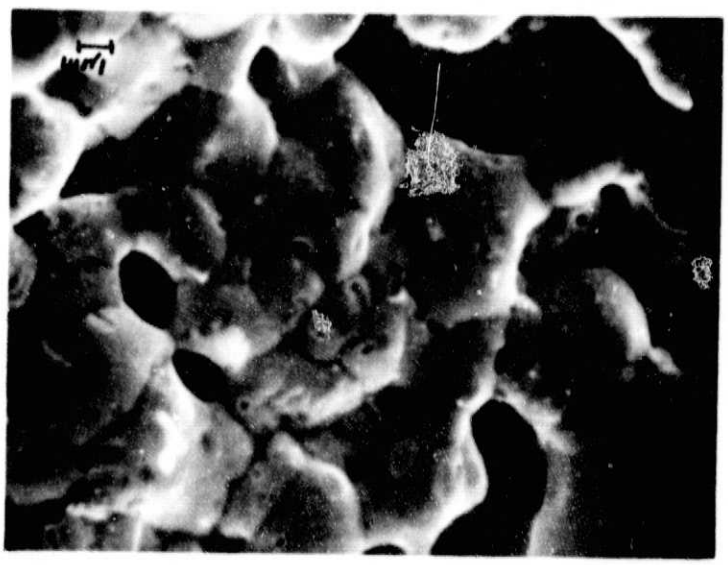

Figure 19. As above except magnification 4200X. Well-knit structure.

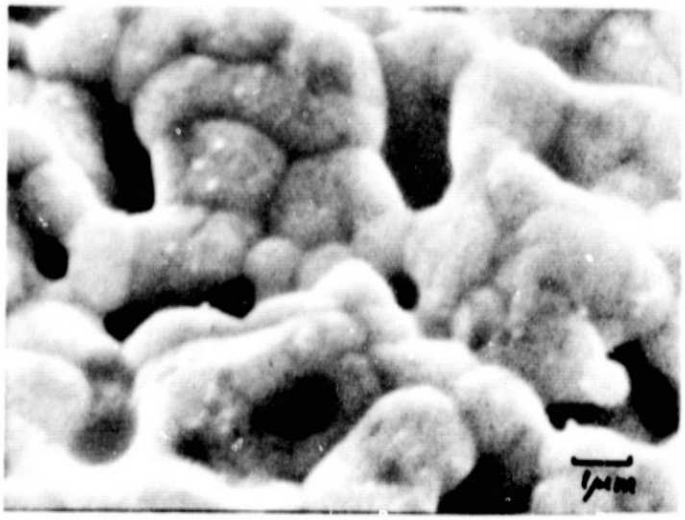

Figure 20. Solar cell metallization with conventional fritted silver ink done with Cambridge SEM at 8000X magnification.

A number of temperature runs were made on S018 (5 wt% AgF, 3 wt% H_3BO_3) to observe sintering action and attendant grain growth as a function of temperature. The belt speed was held constant throughout the experiment and previously printed wafers were fired at 50°C intervals from 500°C to 750°C. All specimens were analyzed with an SEM at 3000X magnification. Unfortunately, a malfunction in the SEM produced images of poor quality, but the salient features of the effect of temperature increase on the grain size and fit are strikingly shown in Figure 21 a,b,c,d,e, and f. It is shown that there is an apparent reversal at 750°C in the trend in going from Figure 21a at 700°C to Figure 21f at 750°C. Since it is unlikely that the samples were interchanged, it is assumed that the grain size was in saturation, and the anomaly is due to local variations in screening parameters--possibly a site near the edge of a pad.

While this may be another example of a matured, all metal, sintered contact, it is possible that the boric acid doping agent serves the dual function of doping agent and non-metal liquid sintering medium. This comes about due to the large ratio in densities of silver/boric acid which increase the atomic percentage to 22 at%.

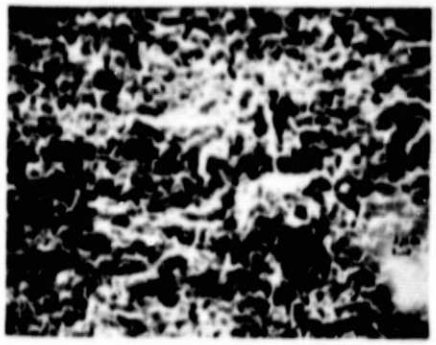

(a)

(b)

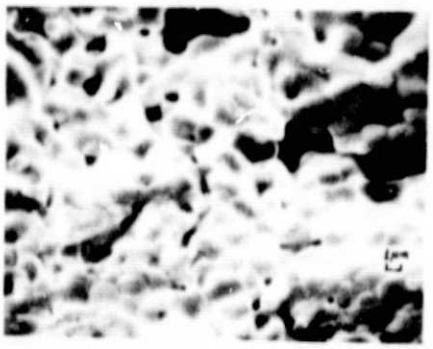

(c)

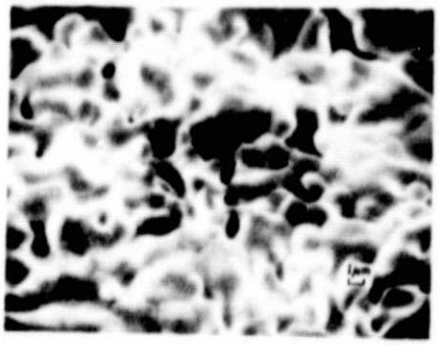

(d)

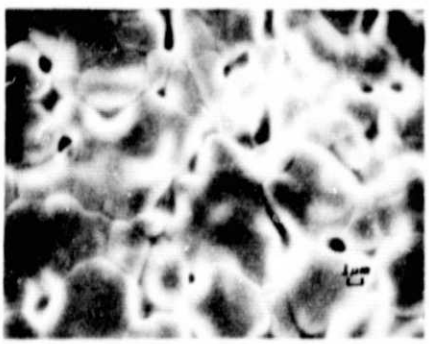

(e)

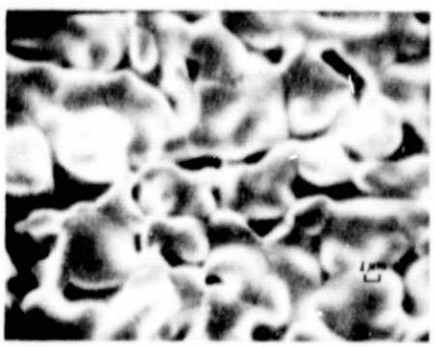

(f)

Figure 21. a) Paste S018 (with 5 wt% AgF and 3 wt% H_3BO_3) on silicon substrate, magnification 3000X, belt speed 12 cm/min, fired at 500°C b) same as (a) except fired at 550 C° c) same as (a) except fired at 600°C d) same as (a) except fired at 650°C e) same as (a) except fired at 700°C f) same as (a) except fired at 750°C.

In order to determine whether the silicon surface is attacked by the hot fluorine gas during the silver fluoride decomposition, we cleaved several printed, fired silicon strips. The paste, S012, was chosen to contain 10 wt% of silver fluoride and was fired at 750°C to exaggerate the effect. Wafers were scribed and broken along the (110) plane both in room temperature air and under liquid nitrogen, to forestall smearing of the silver-silicon interface. The room temperature cleave gave a cleaner profile, with the results shown in Figure 22 a,b,c. (A) shows the edge of the print (toward the right side of the photo) at 1150X magnification. Due to the lacy nature of sintered paste contacts there are several areas at the edge where the silicon is not covered with silver. This results in highlighting or haloing the edge which is, in fact, a diffraction effect, but cannot be ascribed to a penetration since the silver fluoride is specifically absent from those areas.

The rectangle in Figure 22a shows the portion enlarged in Figure 22b and 5700X. An empty spot exists at the lower left extreme of the photo. Similarly, a rectangle shows the field of view seen in Figure 22c at 11,500X. Since the smallest distances that can be clearly resolved in this photo are less than 0.1μm, there do not appear to be any macroscopic penetrations into the silicon surface in the vicinity of the pad. Ten such areas were examined with similar results.

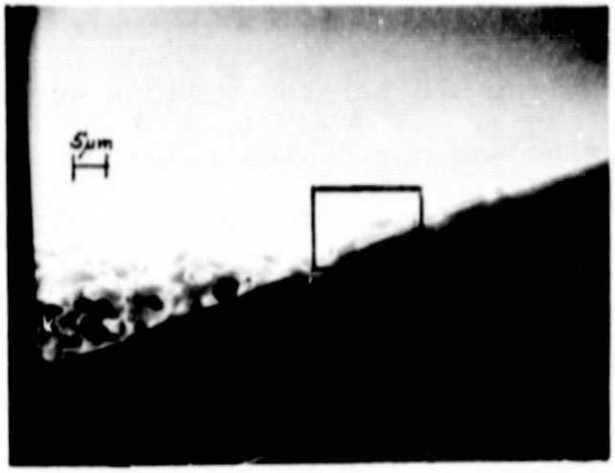

(a)

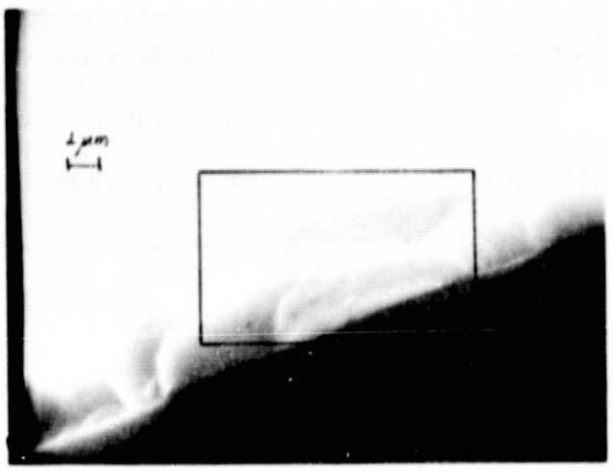

(b)

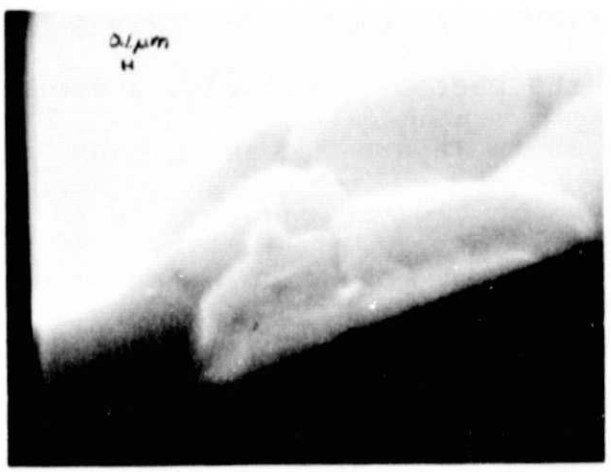

(c)

Figure 22. a) Profile of room temperature cleaved silicon printed with silver paste S 012 containing 10 wt% AgF fired at 750°C, beltspeed 12 cm/min at 1150X magnification. Rectangle indicates area covered by b) 5700X magnification. Rectangle indicates area covered by c) 11,500X magnification.

13.0 Electrical Characteristics

None of the silver electrodes resulting from the various pastes applied to N-type silicon gave linear or ohmic current-voltage behavior. Low voltage resistance between pads 0.1" square with a separation of 0.050" gave in the tens of megohms. Wafer thickness and resistivity were 0.020" and 5Ωcm. Similar results were seen for P-type material with wafer resistivity 1-3Ωcm.

Curve traces of pairs of electrodes resulted in very horizontal regions near the origins, symmetrically disposed and steepening to read 0.5 mA at 4 volts. While the contacts were not ohmic, they did not represent good Schottky barriers, but were rather somewhere between. This was found during several attempts to obtain a definitive barrier height. During one such attempt, we tried to measure the capacitance versus bias voltage on a small signal 1 MHz capacitance bridge. The results, when plotted as $1/C_v^2$ (where C_v is the capacitance in picofarads) against the applied bias voltage (V) did not yield the expected straight line whose slope specifies the carrier concentration and whose intercept provides the Schottky diode internal voltage. A further try was performed by Rockwell International Science Center, Thousand Oaks, California through the kindness of Dr. Marshall Cohen,with similar results, presumably for the same reasons. Small square pads $(.05cm)^2$ measured in this fashion gave approximately 120 pF capacitance or 0.05 $\mu F/cm^2$.

To reduce the leaky Schottky barrier , the paste (S018) discussed in the previous section (3. Further Experiments) was prepared

with a boron addition. The results of the measurements were variable, yielding a reduction in resistance for some electrodes of three orders of magnitude and for others of only one.

14.0 Conclusions and Problems

Good metallurgical contacts have been produced on silicon substrates utilizing all metal ink pastes including 5 wt% (solids) silver fluoride. The basic concept of all metal or glass fritless inks has been demonstrated in the silver system. This can be done at temperatures of 700°to 750°C, without the use of a low melting metal component providing a liquid sintering medium, due to the fine grain metallic silver furnished by decomposing silver fluoride. The silver fluoride wetting action on the freshly etched silicon surface gives contacts with excellent adhesion.

Three solid materials capable of removing SiO_2 from silicon at moderate temperatures have been found. While both Teflon^R and ammonium fluoride-bifluoride effectively remove silica, poor adhesions results when they are used in silver pastes. We believe this to be due to the activation temperatures being too far from the ink sintering temperatures. This causes the silicon to re-oxidize before the silver has a chance to wet it. Electrically, silver deposited from silver fluoride appears to create a leaky Schottky barrier, resulting in non-ohmic contacts.

Considerable difficulties were experienced due to shipping delays by suppliers of silver fluoride, or because of receipt of inferior product, usually caused by inadequate packaging. This caused the silver fluoride to be wet upon arrival and rendered it unusable. The supplier believes he has corrected this problem.

15.0 Plans and Recommendations

During the next quarter the following efforts will be made:

1. Experiments with all metal pastes including low melting point metal components to achieve firing temperatures in the 550°C to 650°C range.
2. Experiments with all metal pastes with ingredients designed to produce good ohmic contacts to N and P-type silicon substrates of modest resistivity.
3. Solar cells will be screened with all metal pastes judged to be the best produced to date, to determine the extent of problems yet remaining.
4. Generation of cost data.
5. Continued efforts with manufacturers and vendors of silver fluoride.

REFERENCES

1. "Constitution of Binary Alloys", M. Hansen and K. Anderko, 2nd edition, page 40, McGraw-Hill, New York, NY,(1958).

2. Handbook of Chemistry and Physics, 56th edition, CRC Press, Cleveland, OH,(1975-1976),Page B-138 S147.

3. Gmelin's Handbuch der Anorganischen Chemie 8. Aufl. Teil B3, page 146 (1973).

4. H.C. Urey, The Merck Index, page 948, 8th edition, P.G. Stecher, Ed. Merck & Co. (1968).

5. I.A. Aksay C.F. Hoge, J.A. Pask, J. Phys. Chem. 78, page 1178, (4).

6. K.F. Zmbov and J.L. Margrave, J. Phys. Chem. 71, page 446, (1967)

16.0 Progress on Program Plan